

## Synthesis and Photophysics of One Mononuclear Mn(III) and One Dinuclear Mn(III,III) Complex Covalently Linked to a Ruthenium(II) Tris(bipyridyl) Complex

Anh Johansson,<sup>†</sup> Malin Abrahamsson,<sup>‡</sup> Ann Magnuson,<sup>§</sup> Ping Huang,<sup>§</sup> Jerker Mårtensson,<sup>||</sup> Stenbjörn Styring,<sup>§</sup> Leif Hammarström,<sup>‡</sup> Licheng Sun,<sup>\*,†</sup> and Björn Åkermark<sup>\*,†</sup>

Department of Organic Chemistry, Stockholm University, S-106 91 Stockholm, Sweden,  
Department of Physical Chemistry, Uppsala University, Box 532, S-751 21 Uppsala, Sweden,  
Department of Biochemistry, Center for Chemistry and Chemical Engineering, University of Lund,  
Box 124, S-221 00 Lund, Sweden, and Department of Organic Chemistry, Chalmers University of  
Technology, 412 96 Göteborg, Sweden

Received May 8, 2003

The preparation of donor (D)–photosensitizer (S) arrays, consisting of a manganese complex as D and a ruthenium tris(bipyridyl) complex as S has been pursued. Two new ruthenium complexes containing coordinating sites for one (**2a**) and two manganese ions (**3a**) were prepared in order to provide models for the donor side of photosystem II in green plants. The manganese coordinating site consists of bridging and terminal phenolate as well as terminal pyridyl ligands. The corresponding ruthenium–manganese complexes, a manganese monomer **2b** and dimer **3b**, were obtained. For the dimer **3b**, our data suggest that intramolecular electron transfer from manganese to photogenerated ruthenium(III) is fast,  $k_{ET} > 5 \times 10^7 \text{ s}^{-1}$ .

### Introduction

In green plants and cyanobacteria, a complicated enzyme system, photosystem II (PS II), is the important part of the photosynthetic apparatus, where water oxidation takes place. This remarkable process, where electrons are extracted from water and molecular oxygen is formed, is essentially a four-electron-oxidation reaction. It takes place in a catalytic center known as the oxygen-evolving complex. This contains a cluster of four manganese ions cycling through five oxidation states, denoted as  $S_0$ – $S_4$ .<sup>1</sup> Close to the manganese cluster is a tyrosine residue<sup>2</sup> believed to be involved in electron–proton,<sup>3</sup> or hydrogen atom,<sup>4</sup> transfer from a water molecule bound to manganese.

The discovery that the tyrosine may play an important role in water oxidation has stimulated the synthesis of new manganese complexes containing phenolate ligands<sup>5</sup> and also of model systems for PS II that contain ruthenium(II) tris(bipyridyl) complexes connected to tyrosine and phenolate ligands that can coordinate manganese.<sup>6,7</sup>

In an effort to make diads and triads of transition-metal complexes that mimic the electron donor side of PS II, we have linked monomeric manganese complexes and a tyrosine unit to a ruthenium(II) tris(bipyridyl) complex,  $[\text{Ru}^{\text{II}}(\text{bpy})_3]$ ,

- (1) (a) Yachandra, V. K.; Sauer, K.; Klein, M. P. *Chem. Rev.* **1996**, *96*, 2927–2950. (b) Britt, R. D. In *Oxygenic Photosynthesis: The Light Reactions*; Ort, D., Yocum, C., Eds.; Kluwer Academic Publishers: Dordrecht, The Netherlands, 1996; pp 137–164. (c) Carrell, T. G.; Tyryshkin, A. M.; Dismukes, G. C. *J. Biol. Inorg. Chem.* **2002**, *7*, 2–22. (d) Dau, H.; Iuzzolino, L.; Dittmer, J. *Biochim. Biophys. Acta* **2001**, *1503*, 24–39. (e) Debus, R. J. *Biochim. Biophys. Acta* **1992**, *1102*, 269–352. (f) Diner, B. A.; Babcock, G. T. In *Oxygenic Photosynthesis: The Light Reactions*; Ort, D., Yocum, C., Eds.; Kluwer Academic Publishers: Dordrecht, The Netherlands, 1996; pp 213–247. (g) Renger, G. *Biochim. Biophys. Acta* **2001**, *1503*, 210–228. (h) Zouni, A.; Witt, H.-T.; Kern, J.; Fromme, P.; Krauss, N.; Saenger, W. *Nature* **2001**, *409*, 739–743.
- (2) (a) Barry, B. A.; Babcock, G. T. *Proc. Natl. Acad. Sci. U.S.A.* **1987**, *84*, 7099–7103. (b) Boerner, R.; Barry, B. A. *J. Biol. Chem.* **1993**, *268*, 17151–17154.
- (3) (a) Gilchrist, M. L., Jr.; Ball, J. A.; Randall, D. W.; Britt, R. D. *Proc. Natl. Acad. Sci. U.S.A.* **1995**, *92*, 9545–9549. (b) Force, D. A.; Randall, D. W.; Britt, R. D. *Biochemistry* **1997**, *36*, 12062–12070.
- (4) (a) Tommos, C.; Tang, X.-S.; Warncke, K.; Hoganson, D. W.; Styring, S.; McCracken, J.; Diner, B. A.; Babcock, G. T. *J. Am. Chem. Soc.* **1995**, *117*, 10325–10335. (b) Hoganson, C. W.; Babcock, G. T. *Science* **1997**, *277*, 1953–1957. (c) Tommos, C.; Babcock, G. T. *Acc. Chem. Res.* **1998**, *31*, 18–25. (d) Diner, B. A.; Force, D. A.; Randall, D. W.; Britt, R. D. *Biochemistry* **1998**, *37*, 17931–17943. (e) Limburg, J.; Szalai, V. A.; Brudvig, G. W. *J. Chem. Soc., Dalton Trans.* **1999**, 1353–1361. (f) Pecoraro, V. L.; Baldwin, M. J.; Caudle, M. T.; Hsieh, W.-Y.; Law, W.-Y.; N. A. *Pure Appl. Chem.* **1998**, *70*, 925–929.

\* Authors to whom correspondence should be addressed. E-mail: licheng.sun@organ.su.se.

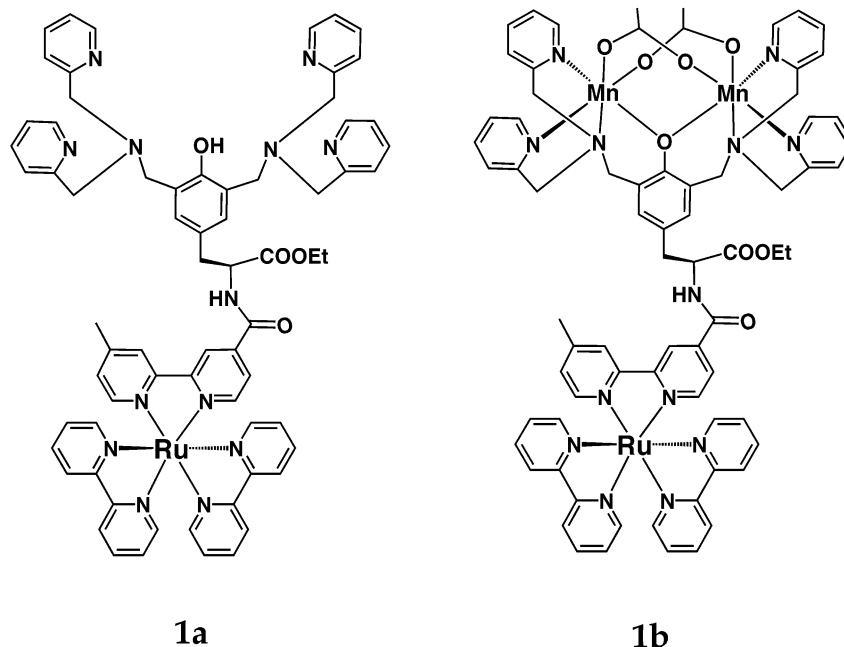
<sup>†</sup> Stockholm University.

<sup>‡</sup> Uppsala University.

<sup>§</sup> University of Lund.

<sup>||</sup> Chalmers University of Technology.

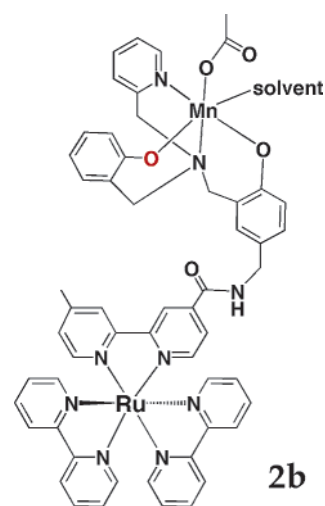
Chart 1



and investigated the excited-state lifetimes and photoinduced electron transfer.<sup>8</sup> For the trinuclear Ru–Mn<sub>2</sub> complex **1b** (Chart 1), where the manganese coordinating site consists of a bridging phenolate and four terminal pyridyl ligands,<sup>6a–c</sup> we have demonstrated that intramolecular electron transfer ( $k_{\text{ET}} > 1 \times 10^7 \text{ s}^{-1}$ ) occurs from Mn<sup>II,II</sup> to the photogenerated ruthenium(III), forming Mn<sup>II,III</sup>.

By using a sacrificial electron acceptor, three steps of photoinduced electron transfer could also be observed and a

Chart 2

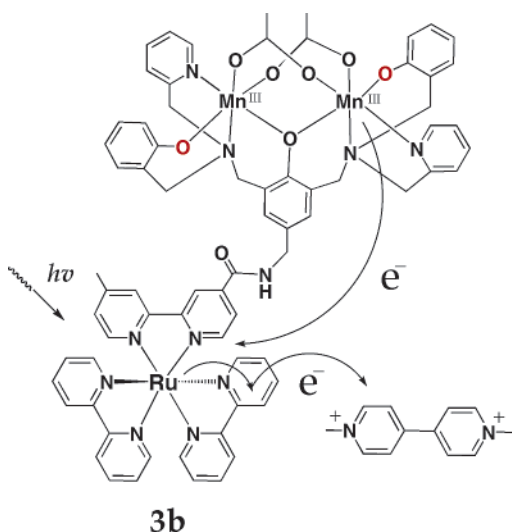


- (5) (a) Horner, O.; Anxolabehere-Mallart, E.; Charlot, M.-F.; Tchertanov, L.; Guilhem, J.; Mattioli, T. A.; Boussac, A.; Girerd, J.-J. *Inorg. Chem.* **1999**, *38*, 1222–1232. (b) Horner, O.; Girerd, J.-J.; Philouze, C.; Tchertanov, L. *Inorg. Chim. Acta* **1999**, *290*, 139–144. (c) Shongwe, M. S.; Mikuriya, M.; Nukada, R.; Ainscough, E. W.; Brodie, A. M.; Waters, J. M. *Inorg. Chim. Acta* **1999**, *290*, 228–236. (d) Lomoth, R.; Huang, P.; Zheng, J.; Sun, L.; Hammarström, L.; Åkermark, B.; Styring, S. *Eur. J. Inorg. Chem.* **2002**, 2965–2974.
- (6) (a) Sun, L.; Raymond, M. K.; Magnuson, A.; LeGourriérec, D.; Tamm, M.; Abrahamsson, M.; Huang Kenéz, P.; Mårtensson, J.; Stenhagen, G.; Hammarström, L.; Styring, S.; Åkermark, B. *J. Inorg. Biochem.* **2000**, *78*, 15–22. (b) Sun, L.; Burkitt, M.; Tamm, M.; Raymond, M. K.; Abrahamsson, M.; LeGourriérec, D.; Frapart, Y.; Magnuson, A.; Huang-Kenez, P.; Brandt, P.; Tran, A.; Hammarström, L.; Styring, S.; Åkermark, B. *J. Am. Chem. Soc.* **1999**, *121*, 6834–6842. (c) Sun, L.; Åkermark, B.; Hammarström, L.; Styring, S. *Chem. Soc. Rev.* **2001**, *30*, 36–49. (d) Magnuson, A.; Berglund, H.; Korall, P.; Hammarström, L.; Åkermark, B.; Styring, S.; Sun, L. *J. Am. Chem. Soc.* **1997**, *119*, 10720–10725.
- (7) (a) Burdinski, D.; Bothe, E.; Wieghardt, K. *Inorg. Chem.* **2000**, *39*, 105–116. (b) Burdinski, D.; Wieghardt, K.; Steenken, S. *J. Am. Chem. Soc.* **1999**, *121*, 10781–10787.
- (8) (a) Sun, L.; Berglund, H.; Davydov, R.; Börje, A.; Norrby, T.; Philouze, C.; Korall, P.; Berg, K. A.; Tran, A.; Andersson, M.; Stenhagen, G.; Mårtensson, J.; Hammarström, L.; Almgren, M.; Styring, S.; Åkermark, B. *J. Am. Chem. Soc.* **1997**, *119*, 6996–7004. (b) Berglund-Baudin, H.; Sun, L.; Davidov, R.; Sundahl, M.; Styring, S.; Åkermark, B.; Almgren, M.; Hammarström, L. *J. Phys. Chem. A* **1998**, *102*, 2512–2518. (c) Hammarström, L.; Sun, L.; Åkermark, B.; Styring, S. *Biochim. Biophys. Acta* **1998**, *1365*, 193–199. (d) Berg, K. E.; Tran, A.; Raymond, M. K.; Abrahamsson, M.; Wolny, J.; Redon, S.; Andersson, M.; Sun, L.; Styring, S.; Hammarström, L.; Toftlund, H.; Åkermark, B. *Eur. J. Inorg. Chem.* **2001**, 1019–1029. (e) Abrahamsson, M.; Berglund Baudin, H.; Tran, A.; Philouze, C.; Berg, K. E.; Raymond-Johansson, M. K.; Sun, L.; Åkermark, B.; Styring, S.; Hammarström, L. *Inorg. Chem.* **2002**, *41*, 1534–1544.

Mn<sup>III,IV</sup> oxidation state was reached in complex **1b**.<sup>9</sup> Attempts to demonstrate the formation of even higher manganese oxidation states have so far not been successful, at least partly because of oxidation of the ligand as indicated by the formation of some free Mn<sup>II</sup>. To prepare ligands that are more compatible with high oxidation states of manganese, we set out to prepare complexes in which some of the pyridyl groups in **1b** have been replaced by phenolate. In this paper, we report the synthesis of the dinuclear Ru–Mn complex **2b** (Chart 2) and the trinuclear Ru–Mn<sub>2</sub> complex **3b** (Chart 3), which are both related to **1b** but in which one or two pyridines have been replaced by phenolates. As in **1b**, the [Ru<sup>II</sup>(bpy)<sub>3</sub>] and manganese moieties are joined by an amide bond. The amide bonds are expected to impart some rigidity to the complexes by virtue of the double-bond character of

- (9) Huang-Kenez, P.; Magnuson, A.; Lomoth, R.; Abrahamsson, M.; Tamm, M.; Sun, L.; van Rotterdam, B.; Park, J.; Hammarström, L.; Åkermark, B.; Styring, S. *J. Inorg. Biochem.* **2002**, *91*, 159–172.

Chart 3



these bonds. This should favor an extended structure over a folded structure of the complexes and decrease both quenching of the excited  $^3\text{MLCT}$  state of  $\text{Ru}^{\text{II}}$  and direct through-space electron transfer from manganese to the photogenerated  $\text{Ru}^{\text{III}}$ . A second difference between the complex **1b**, on the one hand, and **2b** and **3b**, on the other hand, is that the link that connects the Ru and Mn moieties in **1b** has been shortened in **2b** and **3b**.

Because it was possible to prepare complex **2b** with a mononuclear manganese moiety and **3b** with a dinuclear manganese moiety, it seemed interesting to see whether this difference in binding had an effect on the rate of electron transfer.

Finally, we were interested in comparing the rates of electron transfer from the phenol moieties to photogenerated  $\text{Ru}^{\text{III}}$  in **1a**, where there is a strong hydrogen bond and fast electron transfer, and in **2a** and **3a**. Also in **2a** and **3a** strong hydrogen bonds between the nitrogen functions and the phenolic hydroxy groups should be formed, but the specific involvement of the central phenol is not clear. The effect on the rate of electron transfer is therefore uncertain, and it seemed particularly interesting to see whether there would be a difference with one hydrogen-bonding arm as in **2a** and two as in **3a**.

## Result and Discussion

**Synthesis and Characterization.** The synthesis of **2a** and **3a** started from the same compound, 4-hydroxybenzyl alcohol (Scheme 1). The alcohol was converted to the protected benzylamine **5** by reaction with acetyl chloride, followed by potassium phthalimide. The reaction of 4-hydroxybenzyl alcohol with acetyl chloride served two purposes: first of all, the benzyl alcohol is converted to the corresponding chloride to enable nucleophilic substitution with phthalimide; second, the phenol group is acetylated and prevented from reacting with phthalimide. After substitution with phthalimide, the acetyl group was hydrolyzed under acidic conditions to give the phenol **6**. When basic conditions were used for hydrolysis, either  $\text{NaOH}$  or  $\text{K}_2\text{CO}_3$ , the phthalimide group was partly cleaved. Functionalization in the ortho position-

(s) of the phenol was achieved by formylation via the Duff reaction, by hexamethylenetetramine in trifluoroacetic acid (TFA).<sup>10</sup> Depending on the reaction conditions, it was possible to obtain either the monoformylated (**7**) or diformylated (**10**) phenol. When dry TFA and a large excess (8 equiv) of hexamethylenetetramine were used, diformylation was obtained with only traces of the monoformylated phenol (Scheme 2). Using less hexamethylenetetramine (4 equiv) resulted in a 1:1 mixture of mono- and diformylated phenol, which could be separated by chromatography. When monoformylation was desired, a shorter reaction time and only 2 equiv of the tetramine were used (Scheme 1). Furthermore, there was no need to run the reaction under dry conditions.

To prepare the ligand **9**, reductive amination of the monoformylated phenol **7** with the secondary amine **15** was attempted. The success with this reaction depends on whether the cyanoborohydride would reduce the iminium intermediate before it could react further. To our delight, this reaction worked, although with moderate yield. The yield was improved when the reaction was carried out in the presence of a Lewis acid,  $\text{ZnCl}_2$ .<sup>11</sup> Deprotection by reaction with hydrazine then gave the amine **9**, which is the precursor of the ligand complex **2a**.

Because reductive amination of the diformylated phenol **10** failed to give good yields, a second strategy was designed to introduce the amine **15**. The compound **10** was first reduced to the corresponding alcohol **11** with  $\text{NaBH}_3\text{CN}/\text{ZnCl}_2$  (Scheme 2).<sup>11</sup> As in the reductive amination, the presence of  $\text{ZnCl}_2$  was necessary to obtain good conversion to the corresponding alcohol (the more common reducing agent  $\text{NaBH}_4$  was not applicable in this case because it also reduced the phthalimide group). The alcohol **11** was then chlorinated with thionyl chloride to give **12**. Reaction with **15**, followed by cleavage of phthalimide with hydrazine gave **14**, the precursor to **3a**.

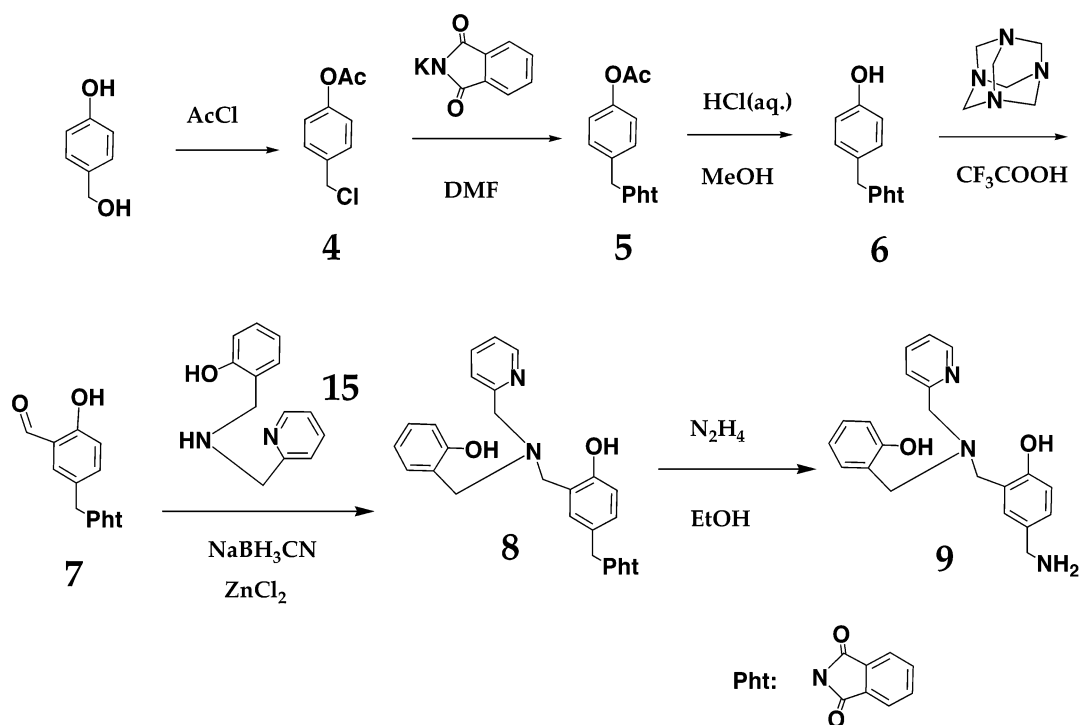
The amines **9** and **14** were then linked to the  $\text{Ru}(\text{bpy})_3$  part via an amide bond to give **2a** and **3a**, respectively (Scheme 3). The Ru–Mn complexes were obtained by reacting **2a** and **3a** with manganese(III) acetate. The electrospray ionization mass spectra (ESI-MS) of **2b** and **3b** showed peaks corresponding to loss of counterion(s) ( $\text{PF}_6^-$ ) (see the Experimental Section).

The complexes were also investigated by cyclic (CV) and differential pulse (DPV) voltammetry. All voltammograms displayed a one-electron oxidation at ca. 1.3 V versus saturated calomel electrode (SCE) and three successive one-electron reductions between  $-1.25$  and  $-1.80$  V, as shown by the DPV peaks for complexes **3a** and **3b** (Figure 1). These can be attributed to the (reversible)  $\text{Ru}^{\text{III/II}}$  oxidation and to the (reversible) reduction of the three bipyridine ligands, respectively. The values of the potential are very similar to the corresponding potentials for  $[\text{Ru}(\text{bpy})_3]^{2+}$ .<sup>12</sup> For **3a**

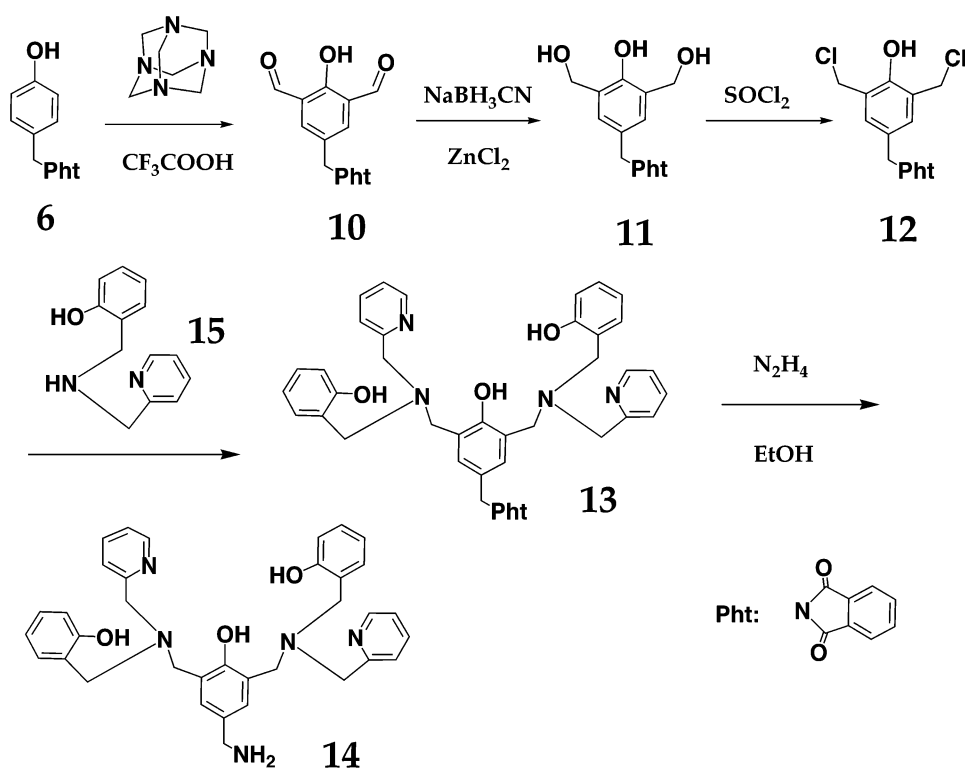
(10) (a) Ogata, Y.; Kawasaki, A.; Sugiura, F. *Tetrahedron* **1968**, *24*, 5001–5010. (b) Lindoy, L. F.; Meehan, G. V.; Svenstrup, N. *Synthesis* **1998**, *7*, 1029–1032.

(11) (a) Kim, S.; Oh, C. H.; Ko, J. S.; Ahn, K. H.; Kim, Y. J. *J. Org. Chem.* **1985**, *50*, 1927–1932. (b) Lane, C. F. *Synthesis* **1975**, *3*, 135–146.

Scheme 1



Scheme 2



additional, irreversible oxidations occurred at  $E_{\text{peak}}$  of ca. 1.05 V in the CV, and in the DPV (Figure 1), additional peaks at ca. 1.05 and 1.26 V, below that of the  $\text{Ru}^{\text{III/II}}$  couple, can be seen. For **2a**, corresponding peaks appeared at the same potentials in the CV and DPV. Similar peaks were earlier observed for **1a**.<sup>6b</sup> We attribute these peaks to oxidation of

the amine and phenolate ligand functions, and the amine oxidation probably occurs at lower potentials than the phenol oxidation.

These ligand oxidation peaks were completely absent in **2b** and **3b**, as expected when manganese is coordinated to the ligands. In **2b**, we could not detect any additional redox processes attributable to the reduction or oxidation of  $\text{Mn}^{\text{III}}$ . In the DPV of **3b**, two small oxidation peaks that were not

(12) Tokel-Takvoryan, N. E.; Hemmingway, N. E.; Bard, A. J. *J. Am. Chem. Soc.* **1973**, *95*, 6582–6589.

Scheme 3

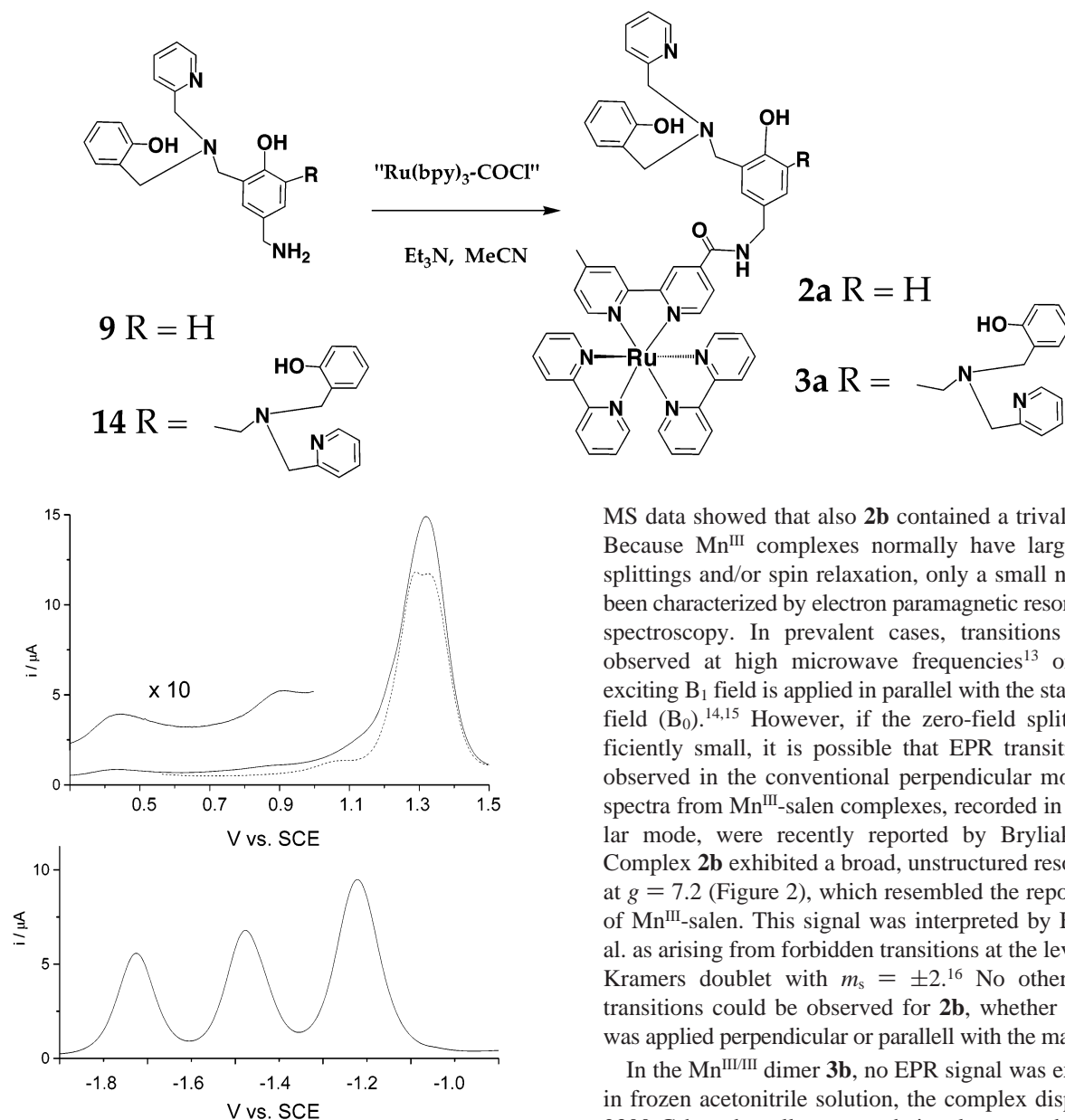


**Figure 1.** DPV data for **3b** (solid) and **3a** (dotted). Conditions: 1 mM **3b** (or **3a**) and 0.1 M TBAPF<sub>6</sub> in dry acetonitrile (see the Experimental Section).

present for **3a** were seen at ca. 0.45 and 0.90 V (Figure 1). In a very similar Mn dimer with di-*tert*-butyl-substituted phenolates that was not linked to a Ru complex, we observed four one-electron-redox processes between  $-0.3$  and  $+1.2$  V, of which at least three were manganese centered.<sup>5d</sup> It is thus possible that the two additional DPV peaks for **3b** arise from oxidation of the manganese complex moiety. By comparison with the results in ref 5d, we expect  $\text{Mn}_2^{\text{II,III}} \rightarrow \text{Mn}_2^{\text{III,III}}$  and  $\text{Mn}_2^{\text{III,III}} \rightarrow \text{Mn}_2^{\text{III,IV}}$  oxidations to occur in this potential range. We have no clear explanation for the poor electrochemical response of the Mn dimer. We note, however, that difficulties in observing manganese redox processes in electrochemical experiments have been reported before, when manganese complexes were linked to Ru complexes.<sup>7</sup>

From the ESI-MS measurements and elemental analysis, it could be concluded that **3b** is a  $\text{Mn}^{\text{III,III}}$  complex. The ESI-

MS data showed that also **2b** contained a trivalent Mn ion. Because  $\text{Mn}^{\text{III}}$  complexes normally have large zero-field splittings and/or spin relaxation, only a small number have been characterized by electron paramagnetic resonance (EPR) spectroscopy. In prevalent cases, transitions have been observed at high microwave frequencies<sup>13</sup> or when the exciting  $B_1$  field is applied in parallel with the static magnetic field ( $B_0$ ).<sup>14,15</sup> However, if the zero-field splitting is sufficiently small, it is possible that EPR transitions can be observed in the conventional perpendicular mode. X-band spectra from  $\text{Mn}^{\text{III}}$ -salen complexes, recorded in perpendicular mode, were recently reported by Bryliakov et al.<sup>16</sup> Complex **2b** exhibited a broad, unstructured resonance peak at  $g = 7.2$  (Figure 2), which resembled the reported spectra of  $\text{Mn}^{\text{III}}$ -salen. This signal was interpreted by Bryliakov et al. as arising from forbidden transitions at the level of a non-Kramers doublet with  $m_s = \pm 2$ .<sup>16</sup> No other signals or transitions could be observed for **2b**, whether the  $B_1$  field was applied perpendicular or parallel with the magnetic field.

In the  $\text{Mn}^{\text{II,III}}$  dimer **3b**, no EPR signal was expected, but in frozen acetonitrile solution, the complex displayed a ca. 2300 G broad, well-structured signal, centered around  $g = 2$ . The signal is characteristic for magnetically coupled, dimeric Mn complexes in the mixed-valence  $\text{Mn}^{\text{II,III}}$  state (see, e.g., ref 17). It therefore clearly contains some mixed-valence  $\text{Mn}^{\text{II,III}}$ . Because the analytical data for **3b** are in very good agreement with a  $\text{Mn}^{\text{III,III}}$  composition, it is unlikely that there are more than a few percent of  $\text{Mn}^{\text{II,III}}$  species in the synthetic samples. A rough quantification of the amount of mixed-valence complexes could be made by

- (13) Goldberg, D. P.; Telser, J.; Krzystek, J.; Montalban, A. G.; Brunel, L.-C.; Barrett, A. G. M.; Hoffman, B. M. *J. Am. Chem. Soc.* **1997**, *119*, 8722–8723.
- (14) Britt, R. D.; Peloquin, J. M.; Campbell, K. A. *Annu. Rev. Biophys. Biomol. Struct.* **2000**, *29*, 463–495.
- (15) Campbell, K. A.; Yikilmaz, E.; Grant, C. V.; Gregor, W.; Miller, A. F.; Britt, R. D. *J. Am. Chem. Soc.* **1999**, *121*, 4714–4715.
- (16) Bryliakov, K. P.; Babushkin, D. E.; Talsi, E. P. *Mendeleev Commun.* **1999**, *1*, 29–32.
- (17) Diril, H.; Chang, H.-R.; Nilges, M. J.; Zhang, X.; Potenza, J. A.; Schugar, H. J.; Isied, S. S.; Hendrickson, D. N. *J. Am. Chem. Soc.* **1989**, *111*, 5102–5114.



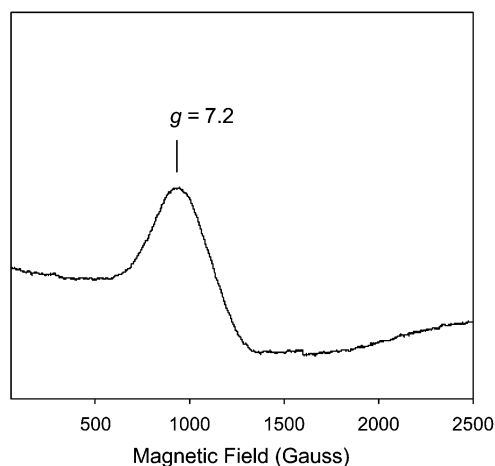


**Figure 2.** X-band EPR spectrum of **2b** in a frozen acetonitrile solution. EPR parameters: microwave frequency, 9.59 GHz; modulation amplitude, 10 G; microwave power, 32 mW; sweep time, 164 s.

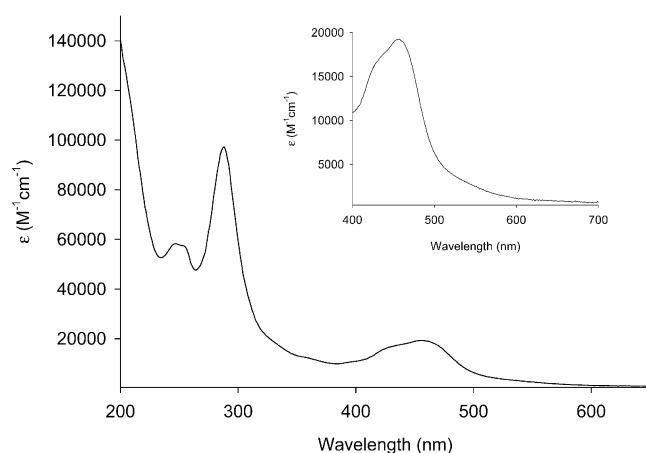


**Figure 3.** Electronic absorption spectrum for **3b** in acetonitrile. The inset shows a magnification of the visible region.

comparison with the EPR ground-state  $S = 1/2$  spectrum of the well-known  $\text{Mn}_2^{\text{II,III}}$ -BPMP complex.<sup>9,17</sup> The two EPR signals are not identical but are very similar. Comparing the signals of **3b** and the  $\text{Mn}_2$ -BPMP complex supported the conclusion that only a few percent of the complex was in the mixed-valence state, and this was also supported by the emission lifetime data (see below).

**Optical Absorption and Emission Properties.** The absorption spectra of **2a** and **3a** in acetonitrile are nearly identical with that of  $[\text{Ru}(\text{bpy})_3]^{2+}$  in the region 300–800 nm.<sup>18</sup> The visible region is dominated by the metal-to-ligand charge transfer (<sup>1</sup>MLCT) band around 455 nm, with an extinction coefficient of ca.  $1.4 \times 10^4 \text{ M}^{-1} \text{ cm}^{-1}$ . The spectra of **2b** and **3b** show some additional absorption contribution from the manganese complex moieties, with an extinction coefficient of ca.  $1.9 \times 10^4 \text{ M}^{-1} \text{ cm}^{-1}$  around 455 nm for **3b** (Figure 3). This absorption contribution is higher in the UV region and decreases monotonically with increasing wavelength, without showing any resolvable structure. This is similar to that of a related simple dinuclear manganese complex with di-*tert*-butyl-substituted phenolates.<sup>5d</sup>

Also, the emission spectra and the emission yield from the <sup>3</sup>MLCT state of **2a** and **3a** in deoxygenated acetonitrile

are very similar to that for  $[\text{Ru}(\text{bpy})_3]^{2+}$ . In **2b** and **3b**, however, the manganese apparently quenches the emission to a great extent. The time-resolved emission data show a single-exponential decay with a lifetime of 1300 ns for both **2a** and **3a**. In contrast, the data for **2b** and **3b** both show a lifetime of only 2 ns, consistent with a strong quenching by the manganese moiety. Minor components with longer lifetimes were observed. For **3b**, the <2% with a 25 ns lifetime is tentatively attributed to complexes with the manganese moiety in a  $\text{Mn}_2^{\text{II,III}}$  state (see the EPR section). We have previously reported strong quenching of the ruthenium MLCT state by attached mononuclear  $\text{Mn}^{\text{II}}$  complexes<sup>8d,e</sup> and by the dinuclear  $\text{Mn}_2^{\text{II,III}}$  moiety in **1b**.<sup>6a</sup> In the former case, the quenching was explained by an exchange-type energy transfer to give short-lived manganese excited states.<sup>8e</sup> For **1b**, it is also conceivable that quenching occurred by electron transfer from the  $\text{Mn}_2^{\text{II,III}}$  moiety to the excited Ru(II) (reductive quenching). For **3b**, there are even more mechanistic possibilities in addition to energy transfer because the electrochemical data indicate that both reductive and oxidative quenching are exoergonic. No quenching products were seen after excited-state decay by transient absorption, showing that any electron-transfer products or excited manganese states must rapidly reform the ground-state reactants after quenching.

**Electron Transfer.** All of the complexes investigated were photooxidized in laser flash photolysis experiments in the presence of the external acceptor methyl viologen  $[\text{MV}(\text{PF}_6)_2]$ . Even the short-lived excited states of **2b** and **3b** could be efficiently photooxidized to  $\text{Ru}^{\text{III}}$  if the concentration of viologen was as high as 0.2 M. The reactions were followed by the transient absorption changes.

In complex **2a**, without manganese, the photooxidation products  $\text{MV}^{\bullet+}$  and  $\text{Ru}^{\text{III}}$  recombined in a diffusion-controlled, second-order reaction to reform the ground-state reactants  $\text{MV}^{2+}$  and  $\text{Ru}^{\text{II}}$ . The first reaction half-life under our conditions was ca. 30  $\mu\text{s}$ . The rate of  $\text{Ru}^{\text{II}}$  ground-state recovery at 450 nm was the same as the rate of  $\text{MV}^{\bullet+}$  decay observed at 600 nm (not shown). This implies that electron transfer from the phenolic ligand to  $\text{Ru}^{\text{III}}$  could not compete on that time scale, and we set a limiting value of  $k < 1 \times 10^4 \text{ s}^{-1}$  for this reaction, which is about the same as that for  $\text{Ru}(\text{bpy})_3$  linked to tyrosine.<sup>6d</sup> This is in contrast to the behavior of **1a**, in which the  $\text{Ru}^{\text{II}}$  recovery occurred with  $k > 1 \times 10^7 \text{ s}^{-1}$  and a phenoxy radical was observed by EPR after the reaction.<sup>6b</sup> For **1a**, we explained the rapid electron transfer from the phenolic group by the fact that its proton is hydrogen bonded by the bases of the other groups of the ligand. This facilitated oxidation of the phenolic group, which is coupled to deprotonation.<sup>19</sup> For **3a**, the rate of  $\text{Ru}^{\text{II}}$  recovery is intermediate between these cases:  $k = 2 \times 10^5 \text{ s}^{-1}$ . Thus, the  $\text{Ru}^{\text{II}}$  recovery at 450 nm is much faster than the  $\text{MV}^{\bullet+}$  decay monitored at 600 nm (Figure 4), implying that  $\text{Ru}^{\text{III}}$

(18) (a) Juris, A.; Balzani, V.; Barigelletti, F.; Campagna, S.; Belser, P.; von Zelewsky, A. *Coord. Chem. Rev.* **1988**, *84*, 85–277. (b) Kalysundaraman, K. *Photochemistry of Polypyridine and Porphyrine Complexes*; Academic Press: London, 1992.

(19) Sjödin, M.; Styring, S.; Åkermark, B.; Sun, L.; Hammarström, L. *J. Am. Chem. Soc.* **2000**, *122*, 3932–3936.

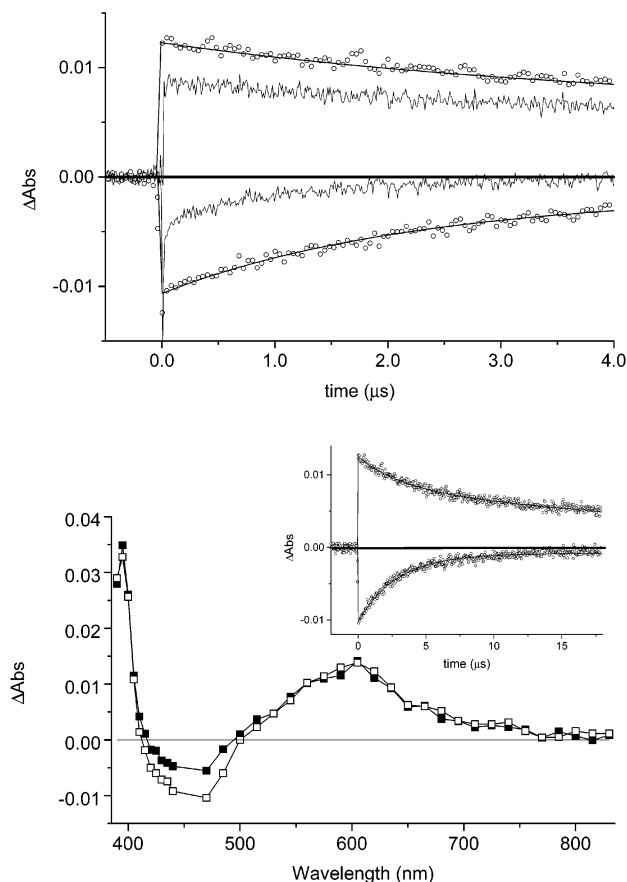


**Figure 4.** Transient absorption changes after excitation at 460 nm for **3a** and **3b** in the presence of 200 mM methyl viologen ( $MV^{2+}$ ): (a) increased absorption at 600 nm due to formation of  $MV^{•+}$  (upper curves) and bleach of the Ru(II) ground state at 470 nm (lower curves) for isoabsorptive solutions of **3a** (circles + line) and **3b** (wiggly line); (b) transient absorption spectra at 100 ns after excitation for **3a** (open squares) and **3b** (solid squares). The spectra were normalized at 600 nm (the **3b** spectrum was multiplied by 1.33) to facilitate comparison of the spectral shapes. Inset: the transient absorption for **3a** at 600 nm (upper curve) and at 470 nm (lower curve) displayed on a longer time scale.

is reduced by electron transfer from the ligand. We suggest that the difference in Ru<sup>II</sup> recovery rates between the complexes can be explained by the different hydrogen-bonding situations. Without a hydrogen bond to the phenolic proton, this cannot deprotonate in acetonitrile, and the potential for the phenol oxidation is then too high to allow oxidation by Ru<sup>III</sup>.<sup>19</sup> This is probably the case in **2a**, and, in fact, NMR of this complex does not indicate the presence of a strong hydrogen bond. In **3a**, the phenolic proton is moderately strongly hydrogen bonded to the ligand, as shown by a proton NMR signal at ca. 9.5 ppm. This facilitates oxidation of the phenol, and the rate of intramolecular oxidation by Ru<sup>III</sup> is higher. Finally, in **1a** there are more potential hydrogen-bonding bases, which makes a stronger hydrogen-bond situation, as is also suggested by the proton NMR signal at 11.5 ppm. This gives the highest electron-transfer rate.

In the manganese-containing complexes, the ligands should be stabilized against oxidation, as is also shown by the electrochemical experiments. Instead, the photogenerated Ru<sup>III</sup> may oxidize the manganese ions. In **2b**, the rates of Ru<sup>II</sup> recovery at 450 nm and  $MV^{•+}$  decay at 600 nm were

very similar (not shown), showing that any electron transfer from Mn<sup>III</sup> to Ru<sup>II</sup> is negligibly slow on that time scale ( $k < 1 \times 10^4 \text{ s}^{-1}$ ). Although the electrochemical data did not give a value for the Mn<sup>III/IV</sup> potential, this may be too high to allow rapid oxidation by Ru<sup>III</sup>.

In **3b**, on the other hand, the Ru<sup>II</sup> recovery was clearly much faster than the  $MV^{•+}$  decay (Figure 4a). From a comparison of the signal amplitudes in Figure 4a, it is clear that most of the Ru<sup>II</sup> recovery occurred within the time resolution of the flash photolysis setup (ca. 10 ns). For **3a**, the magnitude of the initial 450 nm Ru<sup>II</sup> bleach is almost the same as that for the 600 nm  $MV^{•+}$  absorption. In contrast, the 450 nm bleach for **3b** after the initial instrument-limited “spike” is very small compared to the 600 nm absorption (Figure 4b). This shows that ca. 50% of the Ru<sup>II</sup> recovery occurred with  $k > 5 \times 10^7 \text{ s}^{-1}$ . We attribute this to intramolecular electron transfer from the Mn<sub>2</sub><sup>III,III</sup> moiety, most likely generating the Mn<sub>2</sub><sup>III,IV</sup> complex. The remaining, slower Ru<sup>II</sup> recovery seen at 450 nm in Figure 4b occurred with the same rate as that in **3a** ( $k = 2 \times 10^5 \text{ s}^{-1}$ ) and can probably be attributed to complexes in which the manganese ions are (partly) dissociated.<sup>20</sup>

It is important to note that the short-lived (2 ns) excited state of **3b** was indeed efficiently quenched at the high concentration of  $MV^{2+}$  (0.2 M) employed. This is shown by the high yield of  $MV^{•+}$  after each flash, which is ca. 75% of the yield in the experiments with **3a**. Thus, the very rapid Ru<sup>II</sup> recovery must be attributed to **3b**.

We could not observe any transient absorption changes from the manganese moiety of **3b** during the electron-transfer reactions. In Figure 4b, the (normalized) transient spectra of **3b**, after the rapid Ru<sup>II</sup> recovery phase, are compared with those for **3a**. The visible region spectra for both complexes show only the  $MV^{•+}$  absorption peaking at 600 nm and different degrees of a Ru<sup>II</sup> bleach centered at 450 nm. The differences in extinction coefficients between the Mn<sub>2</sub><sup>III,III</sup> and Mn<sub>2</sub><sup>III,IV</sup> states are apparently too small to be resolved in the transient spectra ( $\Delta\text{Abs} \leq 0.001$ ). This is consistent with the spectroelectrochemical data for a manganese dimer that is very similar to the manganese dimer moiety of **3b** but that has di-*tert*-butyl-substituted phenolates ( $\Delta\epsilon \leq 800 \text{ M}^{-1} \text{ cm}^{-1}$  in the visible region).<sup>5d</sup> Nevertheless, the very rapid Ru<sup>II</sup> recovery in **3b**, which is not observed in **3a**, which lacks manganese, strongly suggests that electron transfer from the manganese complex moiety to the photogenerated Ru<sup>III</sup> occurs with a rate constant of  $k > 5 \times 10^7 \text{ s}^{-1}$ .

## Conclusion

Two new ruthenium–manganese complexes have been prepared, one with a mononuclear manganese(III) moiety (**2b**) and one with a dinuclear manganese(III) moiety (**3b**). The manganese moiety and the ruthenium center are linked

(20) We noted that this kinetic component increased in magnitude when the  $MV^{2+}$  concentration was increased above 0.2 M, suggesting that the viologen may cause a partial dissociation of the manganese. This can possibly explain the fact that the relative magnitude of the slower component is much larger than the value obtained from the emission lifetime data.

by an amide bond, designed to impart rigidity to the system. The Ru<sup>II</sup> <sup>3</sup>MLCT excited-state lifetimes of both complexes were very short (ca. 2 ns) because of quenching by the manganese moiety. For **3b**, the transient absorption data indicate that, although the lifetime is short, Ru<sup>II</sup> can be photooxidized to Ru<sup>III</sup> and then rereduced by very fast intramolecular electron transfer from the coordinated manganese ( $k_{ET} > 5 \times 10^7 \text{ s}^{-1}$ ). The lower limit of this rate constant is slightly higher than the one for complex **1b**, which had been studied earlier.

In addition, the rates of intramolecular electron transfer from the phenol to photogenerated Ru<sup>III</sup> in the precursor complexes **1a**, **2a**, and **3a** were found to correlate roughly with the strength of the hydrogen bond to the phenolic hydroxy groups, as indicated by the proton NMR shifts.

## Experimental Section

**General Methods.** The emission and absorption measurements were performed at room temperature in deaerated acetonitrile of spectroscopic grade (Merck, 99.8%). The absorption spectra were recorded on a HP 8453 diode-array spectrophotometer, and the emission spectra were recorded using a SPEX fluorolog II system.

All electrochemistry was performed under argon, and the electrolyte used was 0.1 M tetrabutylammonium hexafluorophosphate (TBAPF<sub>6</sub>) in acetonitrile (Aldrich, 99.8%) that was dried over molecular sieves (3 Å). The salt was dried at 140 °C for more than 48 h before preparation of the electrolyte. CV and DPV were recorded using a three-electrode system consisting of a Ag/AgNO<sub>3</sub> reference electrode (Ag wire in 10 mM AgNO<sub>3</sub> in acetonitrile), a platinum wire as the counter electrode, and a freshly polished glassy carbon (diameter 2 mm) as the working electrode. Both the reference electrode and counter electrode were kept in compartments filled with electrolyte separated from the solution by a salt bridge. Before the compound was dissolved, the electrolyte was purged with argon for 10 min. A potentiostat from Eco Chemie with an Autolab/GPES electrochemical interface was used. The reported half-wave potentials,  $E_{1/2}$  [where  $E_{1/2} = (E_{p,a} + E_{p,c})/2$ ], were measured using ferrocene as an internal reference and converted to SCE scale using the values reported in the work by Pavlishchuk and Addison.<sup>21</sup>

The excited-state lifetimes of all of the compounds were determined using time-correlated single-photon counting; the setup used is described elsewhere.<sup>22</sup> The emission was selected with a 600 nm interference filter (Oriol). Measurements were performed with a multichannel analyzer (512 channels) on several different time scales (from 0.08 to 8 ns per channel) for each sample to correctly evaluate the different emission decay components. All room temperature measurements were performed under nitrogen in degassed acetonitrile of spectroscopic grade (Merck, 99.8%). Low-temperature measurements were performed in butyronitrile (Fluka, 99%) using capillary tubes inserted in a coldfinger Dewar filled with liquid nitrogen.

Transient absorption was studied using a flash photolysis system with a Q-switched Nd:YAG laser ( $\lambda = 355 \text{ nm}$ ) to pump an optical parametric oscillator, delivering <10 ns flashes tunable between 410 and 660 nm. The analyzing light was provided by a pulsed Xe lamp in a spectrometer system from Applied Photophysics. The

samples contained  $\sim 30 \mu\text{M}$  of the complex and  $\sim 40 \text{ mM}$  of MV-(PF<sub>6</sub>)<sub>2</sub>, which was prepared from commercial MVCl<sub>2</sub> (Sigma) by adding aqueous NH<sub>4</sub>PF<sub>6</sub> to precipitate the PF<sub>6</sub> salt. The product was purified by recrystallization from ethanol.

EPR measurements were performed on a Bruker E500 X-band spectrometer equipped with a Bruker 4116 DM dual-mode cavity and an Oxford Instruments ESR900 flow cryostat. Complexes **2b** and **3b** were dissolved to 1 mM in dry acetonitrile and frozen in liquid nitrogen before measurements. Spectrometer settings were as follows: modulation frequency, 100 kHz; modulation amplitude, 10 G. All spectra were taken at a temperature of 4 K. See the figure legends for further details.

<sup>1</sup>H NMR spectra were recorded with a Varian AM 400 MHz spectrometer or a Bruker DMX 500 MHz spectrometer.

The ESI-MS experiments were performed on a ZacSpec mass spectrometer (VG Analytical, Fisons Instrument). Electrospray conditions were as follows: needle potential, 3 kV; acceleration voltage, 4 kV; bath and nebulizing gas, nitrogen.

Elemental analyses were determined by Analytische Laboratorien GMBH, Industriepark Kaiserau, Lindlar, Germany.

**Materials.** Dimethylformamide (DMF) and trifluoroacetic acid were distilled from CaH<sub>2</sub> and phosphorus pentoxide (P<sub>2</sub>O<sub>5</sub>), respectively. Potassium phthalimide was recrystallized from EtOH and washed with acetone. Zinc chloride was recrystallized from dioxane.

**Synthesis. Ruthenium–Manganese Complexes (2b and 3b).** **2b** was synthesized by dissolving **2a** (0.030 g, 0.024 mmol) in 2 mL of MeCN, and 0.1 mL of NaOH (1 M) was added. Then Mn(OAc)<sub>3</sub> (0.012 g, 0.04 mmol) in 1 mL of H<sub>2</sub>O was added, and the resulting solution was stirred at ambient temperature for 18 h. MeCN was evaporated, and MeOH (2 mL) was added. A saturated solution of NH<sub>4</sub>PF<sub>6</sub> was added to precipitate the complex as the PF<sub>6</sub> salt. The brown precipitate was filtered and washed with water. Yield: 0.015 g (46%). ESI-MS ( $m/z$ ): 1216.9 [M – PF<sub>6</sub><sup>–</sup>], 536.4 [M – 2PF<sub>6</sub><sup>–</sup>], 337.3 [M – 2PF<sub>6</sub><sup>–</sup> – OAc<sup>–</sup>].

**Complex 3b** was synthesized by dissolving **3a** (0.050 g, 0.034 mmol) in MeCN (3 mL) and adding 0.1 mL of NaOH (1 M) and Mn(OAc)<sub>3</sub> (0.036 g, 0.12 mmol) in 1 mL of H<sub>2</sub>O. The resulting solution was stirred at ambient temperature for 6 h, and MeCN was evaporated. Amounts of 2 mL of MeOH and saturated NH<sub>4</sub>PF<sub>6</sub>(aq) were added. The brown precipitate was collected by filtration and washed with water. Yield: 0.044 g (70%). ESI-MS ( $m/z$ ): 1701.1 [M – PF<sub>6</sub><sup>–</sup>], 779.0 [M – 2PF<sub>6</sub><sup>–</sup>], 470.8 [M – 3PF<sub>6</sub><sup>–</sup>]. Anal. Calcd for (C<sub>71</sub>H<sub>64</sub>N<sub>11</sub>O<sub>8</sub>RuMn<sub>2</sub>)(3PF<sub>6</sub><sup>–</sup>): C, 46.17; H, 3.60; N, 8.34; Mn, 5.95. Found: C, 46.03; H, 3.66; N, 8.21; Mn, 5.79.

**Complex 2a.** Bis(2,2'-bipyridine)(4'-methyl-2,2'-bipyridine-4'-carboxylic acid)ruthenium bis(hexafluorophosphate)<sup>23</sup> (0.40 g, 0.44 mmol) was refluxed in 3 mL of SOCl<sub>2</sub> for 2 h. Excess of SOCl<sub>2</sub> was removed under reduced pressure. The dry solid was redissolved in 8 mL of dry acetonitrile and cooled in an ice bath. Compound **9** (0.15 g, 0.44 mmol) and triethylamine (0.5 mL) were added, and the resulting solution was stirred under argon for 1 h at 0 °C and 4 h at ambient temperature. Purification on a column of silica gel using MeCN–water–KNO<sub>3</sub>(sat.) (95:4:1) as the eluent gave 0.30 g (54%) of the desired product **2a**. (After chromatography, the solvent was evaporated, the solid dissolved in a minimum amount of MeOH, and the product reprecipitated by addition of saturated NH<sub>4</sub>PF<sub>6</sub>.) <sup>1</sup>H NMR ( $\delta$  ppm, acetone-*d*<sub>6</sub>): 2.60 (s, 3H, CH<sub>3</sub>–), 3.83 (s, 2H, HOPhCH<sub>2</sub>N–), 3.85 (s, 2H, HOPhCH<sub>2</sub>N–), 3.96 (s, 2H, PyCH<sub>2</sub>N–), 4.54 (d,  $J = 5.5 \text{ Hz}$ , 2H, HOPhCH<sub>2</sub>NHCO), 6.71 (d,

(21) Pavlishchuk, V. V.; Addison, A. W. *Inorg. Chim. Acta* **2000**, *298*, 97–102.

(22) Almgren, M.; Hansson, P.; Mukhtar, E.; van Stam, J. *Langmuir* **1992**, *8*, 2405–2412.

(23) Peck, B. M.; Ross, G. T.; Edwards, S. W.; Meyer, G. I.; Meyer, T. J.; Erickson, B. W. *Int. J. Pept. Protein Res.* **1991**, *38*, 114–123.



$J = 8.0$  Hz, 1H, HOPh-*H*), 6.75–6.77 (m, 2H, HOPh-*H*), 7.12 (t,  $J = 7.5$  Hz, 1H, HOPh-*H*), 7.15 (d,  $J = 8.0$  Hz, 1H, HOPh-*H*), 7.19 (d,  $J = 8.0$  Hz, 1H, HOPh-*H*), 7.23 (s, 1H, HOPh-*H*), 7.40–7.43 (m, 2H, Py-*H*), 7.47 (d,  $J = 5.5$  Hz, 1H, bpy'-*H*), 7.55–7.63 (m, 4H, bpy-*H*), 7.87 (dt,  $J = 7.7$  and 1.8 Hz, 1H, Py-*H*), 7.91 (d,  $J = 5.5$  Hz, 2H, bpy'-*H*), 8.05–8.10 (m, 3H, bpy-*H*), 8.13 (d,  $J = 5.5$  Hz, 1H, bpy-*H*), 8.20–8.26 (m, 5H, bpy-*H* and bpy'-*H*), 8.57 (d,  $J = 4.5$  Hz, 1H, Py-*H*), 8.82–8.87 (m, 5H, bpy-*H* and bpy'-*H*), 9.14 (s, 1H, bpy'-*H*). ESI-MS ( $m/z$ ): 1104.0 [M - PF<sub>6</sub><sup>-</sup>], 479.2 [M - 2PF<sub>6</sub><sup>-</sup>].

**Complex 3a.** Bis(2,2'-bipyridine)(4'-methyl-2,2'-bipyridine-4'-carboxylic acid)ruthenium bis(hexafluorophosphate)<sup>23</sup> (0.20 g, 0.22 mmol) was refluxed in 1 mL of SOCl<sub>2</sub> for 2 h. Excess of SOCl<sub>2</sub> was removed under reduced pressure. The dry solid was redissolved in 2 mL of dry acetonitrile and cooled in an ice bath. Compound **14** (0.10 g, 0.22 mmol) and triethylamine (0.5 mL) were added, and the resulting solution was stirred under argon and allowed to reach room temperature overnight. Purification on a column of silica gel using MeCN–water–KNO<sub>3</sub>(sat.) (94:4:2) as the eluent gave 0.16 g (50%) of the desired product **3a**. (After column chromatography, the solvent was evaporated, the solid dissolved in a minimum amount of MeOH, and the product reprecipitated by addition of saturated NH<sub>4</sub>PF<sub>6</sub>.) <sup>1</sup>H NMR ( $\delta$  ppm, acetone-*d*<sub>6</sub>): 2.57 (s, 3H, CH<sub>3</sub>-), 4.00 (s, 4H, HOPhCH<sub>2</sub>N-), 4.03 (s, 4H, HOPhCH<sub>2</sub>N-), 4.09 (s, 4H, PyCH<sub>2</sub>N-), 4.55 (d,  $J = 4.4$  Hz, 2H, HOPhCH<sub>2</sub>NHCO), 6.71 (d,  $J = 8.0$  Hz, 2H, HOPh-*H*), 6.77 (t,  $J = 7.2$  Hz, 2H, HOPh-*H*), 7.12 (t,  $J = 7.9$  Hz, 2H, HOPh-*H*), 7.19 (d,  $J = 7.2$  Hz, 2H, HOPh-*H*), 7.29 (s, 2H, HOPh-*H*), 7.34–7.38 (m, 4H, Py-*H*), 7.45 (d,  $J = 5.1$  Hz, 1H, bpy'-*H*), 7.51–7.60 (m, 4H, bpy-*H*), 7.91 (dt,  $J = 7.7$  and 1.5 Hz, Py-*H*), 7.88 (d,  $J = 5.8$  Hz, 1H, bpy'-*H*), 7.92 (dd,  $J = 5.8$  and 1.5 Hz, 1H, bpy'-*H*), 8.03–8.04 (m, 3H, bpy-*H*), 8.10 (d,  $J = 5.5$  Hz, 1H, bpy-*H*), 8.17–8.24 (m, 5H, bpy-*H* and bpy'-*H*), 8.57 (d,  $J = 4.4$  Hz, 2H, Py-*H*), 8.78–8.82 (m, 5H, bpy-*H* and bpy'-*H*), 9.11 (s, 1H, bpy'-*H*). ESI-MS ( $m/z$ ): 1329.8 [M - PF<sub>6</sub><sup>-</sup>], 592.2 [M - 2PF<sub>6</sub><sup>-</sup>].

**4-(Chloromethyl)phenyl Acetate (4).** Compound **4** was prepared according to a procedure described by Taylor et al.<sup>24</sup> *p*-Hydroxybenzyl alcohol (5.0 g, 0.040 mol) was added in small portions to a stirred solution of acetyl chloride (20 mL). The addition was done at such a rate so as to keep the evolution of HCl gas at a moderate rate. The resulting solution was stirred at ambient temperature overnight. Excess of acetyl chloride was removed with a water pump. The resulting liquid was diluted with 50 mL of Et<sub>2</sub>O and then treated with a saturated solution of NaHCO<sub>3</sub>. After the CO<sub>2</sub> evolution had ceased, the solution was transferred to a separatory funnel and the organic phase was separated. The aqueous phase was extracted with Et<sub>2</sub>O (2 × 25 mL). The combined organic phase was washed with brine (2 × 50 mL) and dried over MgSO<sub>4</sub>. Removal of solvent gave 6.4 g of **4** as a pale yellow liquid. Yield: 86%. <sup>1</sup>H NMR ( $\delta$  ppm, CDCl<sub>3</sub>): 2.30 (s, 3H, CH<sub>3</sub>COOPh-), 4.58 (s, 2H, CH<sub>3</sub>COOPhCH<sub>2</sub>Cl), 7.09 (d,  $J = 8.9$  Hz, 2H, CH<sub>3</sub>COOPh-*H*), 7.40 (d,  $J = 8.9$  Hz, 2H, CH<sub>3</sub>COOPh-*H*).

**2-(4-Acetoxybenzyl)isoindole-1,3-dione (5).** A solution of **4** (6.3 g, 0.034 mol) and potassium phthalimide (7.5 g, 0.041 mol) in 50 mL of DMF was heated at 80 °C for 3 h under nitrogen. The cooled reaction mixture was diluted with 70 mL of CHCl<sub>3</sub>, and 100 mL of water was added. The organic phase was separated, and the aqueous phase was extracted with CHCl<sub>3</sub>. The combined organic phase was washed with cold 0.1 M NaOH (50 mL) and water (2 ×

50 mL). The solvent was evaporated until a white solid started to precipitate. A total of 100 mL of Et<sub>2</sub>O was added to get complete precipitation. After 1 h, the solid was collected by suction filtration, washed with Et<sub>2</sub>O, and dried to give 8.1 g (80%) of product **5**. Mp: 164–165 °C. <sup>1</sup>H NMR ( $\delta$  ppm, CDCl<sub>3</sub>): 2.30 (s, 3H, CH<sub>3</sub>COOPh-), 4.83 (s, 2H, CH<sub>3</sub>COOPhCH<sub>2</sub>Pht), 7.03 (d,  $J = 8.9$  Hz, 2H, CH<sub>3</sub>COOPh-*H*), 7.47 (d,  $J = 8.9$  Hz, 2H, CH<sub>3</sub>COOPh-*H*), 7.69–7.73 (m, 2H, CH<sub>3</sub>COOPhCH<sub>2</sub>Pht-*H*), 7.83–7.85 (m, 2H, CH<sub>3</sub>COOPhCH<sub>2</sub>Pht-*H*).

**2-(4-Hydroxybenzyl)isoindole-1,3-dione (6).** Compound **5** (10 g) was suspended in 50 mL of MeOH and 100 mL of 2 M HCl. The solution was heated at 70 °C overnight. The reaction mixture was cooled and filtered. The white precipitate was washed with water and dried to give 8.2 g (97%) of **6**. Mp: 204 °C. <sup>1</sup>H NMR ( $\delta$  ppm, DMSO-*d*<sub>6</sub>): 4.64 (s, 2H, HOPhCH<sub>2</sub>Pht), 6.68 (d,  $J = 8.5$  Hz, 2H, HOPh-*H*), 7.11 (d,  $J = 8.5$  Hz, 2H, HOPh-*H*), 7.83–7.90 (m, 4H, HOPhCH<sub>2</sub>Pht-*H*).

**5-(1,3-Dioxo-1,3-dihydroisoindol-2-ylmethyl)-2-hydroxybenzaldehyde (7).** This compound was prepared according to the modification of a procedure described by Lindoy et al.<sup>10b</sup> The protected phenol **6** (0.50 g, 2.0 mmol) and hexamethylenetetramine (0.55 g, 4.0 mmol) were dissolved in 10 mL of trifluoroacetic acid, and the resulting yellow solution was refluxed for 19 h. The reaction mixture was then poured into 50 mL of HCl (4 M) and stirred for 40 min. The acidic solution was extracted with CH<sub>2</sub>Cl<sub>2</sub> (3 × 20 mL). The combined organic phase was washed with 4 M HCl (2 × 20 mL) and brine (2 × 20 mL). Purification on a short column of silica gel using CH<sub>2</sub>Cl<sub>2</sub> as the eluent gave 0.35 g (64%) of the desired product **7**. <sup>1</sup>H NMR ( $\delta$  ppm, DMSO-*d*<sub>6</sub>): 4.71 (s, 2H, HOPhCH<sub>2</sub>Pht), 6.96 (d,  $J = 8.5$  Hz, 1H, HOPh-*H*), 7.48 (dd,  $J = 8.5$  and 2.2 Hz, 1H, HOPh-*H*), 7.58 (d,  $J = 2.2$  Hz, 1H, HOPh-*H*), 7.84–7.91 (m, 4H, HOPhCH<sub>2</sub>Pht-*H*), 10.2 (s, 1H, HOPhCO-*H*).

**2-{4-Hydroxy-3-[(2-hydroxybenzyl)(pyridin-2-ylmethyl)amino]methyl}benzyl}isoindole-1,3-dione (8).** Aldehyde **7** (0.20 g, 0.71 mmol), (2-hydroxybenzyl)(2-pyridylmethyl)amine (**15**; 0.30 g, 1.4 mmol), NaBH<sub>3</sub>CN (0.044 g, 0.71 mmol), and ZnCl<sub>2</sub> (0.050 g, 0.37 mmol) were suspended in 10 mL of MeOH. The yellow solution was stirred at room temperature overnight. A few drops of concentrated HCl was added to the orange solution to decompose any remaining NaBH<sub>3</sub>CN. The solvent was evaporated under reduced pressure. The resulting solid was dissolved in CH<sub>2</sub>Cl<sub>2</sub> (25 mL) and washed with water (20 mL), and the solvent was removed under reduced pressure. The crude product was purified on a column of silica gel using EtOAc–pentane (1:1) as the eluent. The product **8** was eluted as the second band. Yield: 0.20 g (59%). <sup>1</sup>H NMR ( $\delta$  ppm, DMSO-*d*<sub>6</sub>): 3.58 (s, 2H, HOPhCH<sub>2</sub>N-), 3.59 (s, 2H, HOPhCH<sub>2</sub>N-), 3.68 (s, 2H, PyCH<sub>2</sub>N-), 4.62 (s, 2H, HOPhCH<sub>2</sub>Pht), 6.64–6.70 (m, 3H, HOPh-*H*), 6.98–7.05 (m, 2H, HOPh-*H*), 7.10–7.14 (m, 2H, HOPh-*H*), 7.24–7.27 (m, 1H, Py-*H*), 7.33 (d,  $J = 7.7$  Hz, 1H, Py-*H*), 7.73 (dt,  $J = 7.7$  and 1.8 Hz, 1H, Py-*H*), 7.82–7.89 (m, 4H, HOPhCH<sub>2</sub>Pht-*H*), 8.46 (m, 1H, Py-*H*), 10.1 (br s, 2H, HOPh-*H*).

**4-(Aminomethyl)-2-[(2-hydroxybenzyl)(pyridin-2-ylmethyl)amino]methyl}phenol (9).** Compound **8** (1.0 g, 2.1 mmol) was suspended in 15 mL of EtOH, and hydrazine hydrate (0.21 g, 4.5 mmol) was added. The solution was refluxed for 2 h and stirred at ambient temperature overnight. The solvent was evaporated under reduced pressure and the resulting solid treated with 30 mL of NaOH (2 M). After stirring for 45 min, the basic solution was neutralized with 2 M HCl, then extracted with CH<sub>2</sub>Cl<sub>2</sub> (3 × 20 mL), and dried over Na<sub>2</sub>SO<sub>4</sub>. Evaporation of solvent yielded 0.56 g (76%) of the product **9**. <sup>1</sup>H NMR ( $\delta$  ppm, DMSO-*d*<sub>6</sub>): 3.57 (s,

(24) Taylor, L. D.; Grasshoff, J. M.; Pluhar, M. *J. Org. Chem.* **1978**, *43*, 1197–1200.

2H, HOPhCH<sub>2</sub>NH<sub>2</sub>), 3.65 (s, 2H, HOPhCH<sub>2</sub>N<sup>-</sup>), 3.66 (s, 2H, HOPhCH<sub>2</sub>N<sup>-</sup>), 3.75 (s, 2H, PyCH<sub>2</sub>N<sup>-</sup>), 6.67–6.76 (m, 3H, HOPh-H), 7.03–7.10 (m, 2H, HOPh-H), 7.10 (s, 1H, HOPh-H), 7.19 (d, *J* = 7.4 Hz, HOPh-H), 7.30–7.33 (m, 1H, Py-H), 7.42 (d, *J* = 7.7 Hz, 1H, Py-H), 7.80 (t, *J* = 7.7 Hz, 1H, Py-H), 8.56 (d, *J* = 4.0 Hz, 1H, Py-H).

**5-(1,3-Dioxo-1,3-dihydroisoindol-2-ylmethyl)-2-hydroxybenzene-1,3-dicarbaldehyde (10).** This compound was prepared according to the modification of a procedure described by Lindoy et al.<sup>10b</sup> Compound **6** (0.5 g, 2.0 mmol) and hexamethylenetetramine (2.2 g, 16 mmol) were suspended in 5 mL of trifluoroacetic acid (distilled from P<sub>2</sub>O<sub>5</sub>). The resulting yellow solution was heated at 110 °C for 2 days. The reaction mixture was poured into 50 mL of 4 M HCl and stirred for 3 h. A yellow solid precipitated during the hydrolysis. This was collected by filtration. The crude product was purified by column chromatography (silica gel). The first yellow band, which contained the monoformylated product, was eluted with CH<sub>2</sub>Cl<sub>2</sub>, and the second band, which contained the diformylated product, was eluted with CH<sub>2</sub>Cl<sub>2</sub>–EtOH (95:5). The yield of **10** was 0.41 g (67%). <sup>1</sup>H NMR (δ ppm, DMSO-*d*<sub>6</sub>): 4.81 (s, 2H, HOPhCH<sub>2</sub>Pht), 7.85–7.92 (m, 4H, HOPhCH<sub>2</sub>Pht-H), 7.99 (s, 2H, HOPh-H), 10.2 (s, 2H, HOPhCO-H).

**2-[4-Hydroxy-3,5-bis(hydroxymethyl)benzyl]isoindole-1,3-dione (11).** Compound **10** (0.27 g, 0.87 mmol), NaBH<sub>3</sub>CN (0.11 g, 1.8 mmol), and ZnCl<sub>2</sub> (0.12 g, 0.87 mmol) were suspended in 10 mL of MeOH and stirred at ambient temperature overnight. The reaction mixture became colorless. Half of the solvent was removed under reduced pressure, and 10 mL of HCl (2 M) was added. After stirring for another 30 min, the white precipitate was collected by filtration, washed with water, and dried to yield 0.24 g (88%) of **11**. <sup>1</sup>H NMR (δ ppm, DMSO-*d*<sub>6</sub>): 4.48 (d, *J* = 5.1 Hz, 4H, –PhCH<sub>2</sub>OH), 4.64 (s, 2H, HOPhCH<sub>2</sub>Pht), 5.19 (t, *J* = 5.1 Hz, 2H, –PhCH<sub>2</sub>OH), 7.10 (s, 2H, HOPh-H), 7.82–7.89 (m, 4H, HOPhCH<sub>2</sub>Pht-H), 8.51 (s, 1H, HOPh-).

**2-[3,5-Bis(chloromethyl)-4-hydroxybenzyl]isoindole-1,3-dione (12).** Compound **11** was dissolved in 2 mL of SOCl<sub>2</sub> and stirred at ambient temperature overnight under nitrogen. Excess of SOCl<sub>2</sub> was removed under reduced pressure. The resulting solid was dissolved in 10 mL of CH<sub>2</sub>Cl<sub>2</sub> and washed with water. The organic layer was separated and dried over Na<sub>2</sub>SO<sub>4</sub>, and the solvent was evaporated to give 0.13 g (80%) of the product **12**. <sup>1</sup>H NMR (δ ppm, DMSO-*d*<sub>6</sub>): 4.65 (s, 2H, HOPhCH<sub>2</sub>Pht), 4.74 (s, 4H, –PhCH<sub>2</sub>Cl), 7.28 (s, 2H, HOPh-H), 7.83–7.90 (m, 4H, HOPhCH<sub>2</sub>Pht-H), 9.48 (s, 1H, HOPh-).

**2-[4-Hydroxy-3,5-bis{[(2-hydroxybenzyl)(pyridin-2-ylmethyl)amino]methyl}benzyl]isoindole-1,3-dione (13).** A solution of a mixture of **12**, **15**, and Et<sub>3</sub>N in CH<sub>2</sub>Cl<sub>2</sub> was stirred at ambient temperature for 2 days. The reaction mixture was diluted with CH<sub>2</sub>Cl<sub>2</sub> and washed with brine (2 × 20 mL). The organic phase was dried over Na<sub>2</sub>SO<sub>4</sub> and the solvent evaporated. Purification on silica gel using EtOAc as the eluent gave the desired product **13**. <sup>1</sup>H NMR (δ ppm, DMSO-*d*<sub>6</sub>): 3.60 (s, 8H, HOPhCH<sub>2</sub>N<sup>-</sup>), 3.67

(s, 4H, PyCH<sub>2</sub>N<sup>-</sup>), 4.61 (s, 2H, HOPhCH<sub>2</sub>Pht), 6.62–6.66 (m, 4H, HOPh-H), 6.98–7.04 (m, 2H, HOPh-H), 7.05 (s, 2H, HOPh-H), 7.10 (m, 2H, HOPh-H), 7.21–7.25 (m, 2H, Py-H), 7.29 (d, *J* = 7.7 Hz, 1H, Py-H), 7.73 (dt, *J* = 7.7 and 1.8 Hz, 2H, Py-H), 7.82–7.89 (m, 4H, HOPhCH<sub>2</sub>Pht-H), 8.44–8.46 (m, 2H, Py-H).

**4-(Aminomethyl)-2,6-bis{[(2-hydroxybenzyl)(pyridin-2-ylmethyl)amino]methyl}phenol (14).** Compound **13** (0.52 g, 7.4 mmol) was suspended in 10 mL of EtOH, and hydrazine hydrate (0.22 g, 4.5 mmol) was added. The solution was refluxed for 2 h and stirred at ambient temperature overnight. The solvent was evaporated under reduced pressure and the resulting solid treated with 30 mL of NaOH (2 M). After stirring for 45 min, the basic solution was neutralized with 2 M HCl, then extracted with CH<sub>2</sub>Cl<sub>2</sub> (3 × 20 mL), and dried over Na<sub>2</sub>SO<sub>4</sub>. Evaporation of the solvent yielded 0.36 g (84%) of the product **14**. <sup>1</sup>H NMR (δ ppm, acetone-*d*<sub>6</sub>): 3.77 (s, 4H, HOPhCH<sub>2</sub>N<sup>-</sup>), 3.80 (s, 4H, HOPhCH<sub>2</sub>N<sup>-</sup>), 3.87 (s, 4H, PyCH<sub>2</sub>N<sup>-</sup>), 4.30 (s, 2H, HOPhCH<sub>2</sub>NH<sub>2</sub>), 6.71–6.76 (m, 4H, HOPh-H), 7.07–7.14 (m, 6H, HOPh-H), 7.32–7.38 (m, 4H, Py-H), 7.79 (dt, *J* = 7.7 and 1.9 Hz, 2H, Py-H), 8.61–8.64 (m, 2H, Py-H).

**2-[(2-Pyridylmethyl)amino]methyl}phenol (15).**<sup>25</sup> Salicylaldehyde (4.9 g, 0.040 mol) was dissolved in MeOH (90 mL), and 2-(aminomethyl)pyridine (4.3 g, 0.040 mol) was added dropwise. The resulting solution was stirred for another 2 h at ambient temperature. NaBH<sub>4</sub> (1.5 g, 0.040 mol) was added in small portions. The reaction mixture was stirred for another 45 min, and then the solvent was removed under reduced pressure. To the residue was added 100 mL of water, and the resulting basic solution was neutralized with HCl (2 M). The solution was extracted with CH<sub>2</sub>Cl<sub>2</sub> (3 × 30 mL). The combined organic phase was dried over Na<sub>2</sub>SO<sub>4</sub> and concentrated. Purification on a column of silica gel using EtOAc as the eluent gave 6.8 g (79%) of product **15**. <sup>1</sup>H NMR (δ ppm, acetone-*d*<sub>6</sub>): 3.93 (s, 2H, HOPhCH<sub>2</sub>N<sup>-</sup>), 4.00 (s, 2H, PyCH<sub>2</sub>N<sup>-</sup>), 6.70–6.75 (m, 2H, HOPh-H), 6.99–7.02 (m, 1H, HOPh-H), 7.09–7.14 (m, 1H, HOPh-H), 7.26–7.29 (m, 1H, Py-H), 7.37 (d, *J* = 7.6 Hz, 1H, Py-H), 7.77 (dt, *J* = 7.6 and 1.8 Hz, 2H, Py-H), 8.56–8.58 (m, 2H, Py-H).

**Acknowledgment.** We thank Dr B. van Rotterdam for early EPR measurements on some samples of **3b** and Olof Johansson for measurement of the UV/vis spectrum of **3b**. Financial support for this work was provided by the Swedish Energy Agency, the European TMR program (TMR network C/96-0031), the Knut and Alice Wallenberg Foundation, the Swedish Research Council (VR), and DESS.

IC0344822

(25) Krebs, B.; Schepers, K.; Bremer, B.; Henkel, G.; Althaus, E.; Mueller-Warmuth, W.; Griesar, K.; Haase, W. *Inorg. Chem.* **1994**, *33*, 1907–1914.